POS 513 Cruise Report

R.V. Poseidon cruise no. 513

Dates, Ports: 09.05.2017 (Heraklion, Crete) – 24.05.2017 (Heraklion, Crete)

Research subject: Tephrostratigraphy along the Aegean arc

Chief Scientist: Dr. Armin Freundt, GEOMAR, Kiel

Number of Scientists: 11

Project: Aegean Tephras

Alphabetical list of participating scientists:

Name	Affiliation
Nico Augustin	GEOMAR, Kiel
Jenny Brandstätter	University of Graz, Austria
Kai Fockenberg	GEOMAR, Kiel
Armin Freundt	GEOMAR, Kiel
Thor Hansteen	GEOMAR, Kiel
Boris Karatsolis	University of Athens, Greece
Steffen Kutterolf	GEOMAR, Kiel
Symeon Nasras	University of Athens, Greece
Thorsten Schott	GEOMAR, Kiel
Carina Sievers	GEOMAR, Kiel
Themistoklis Troupakis	Observer, Ephorate for Underwater Archeology

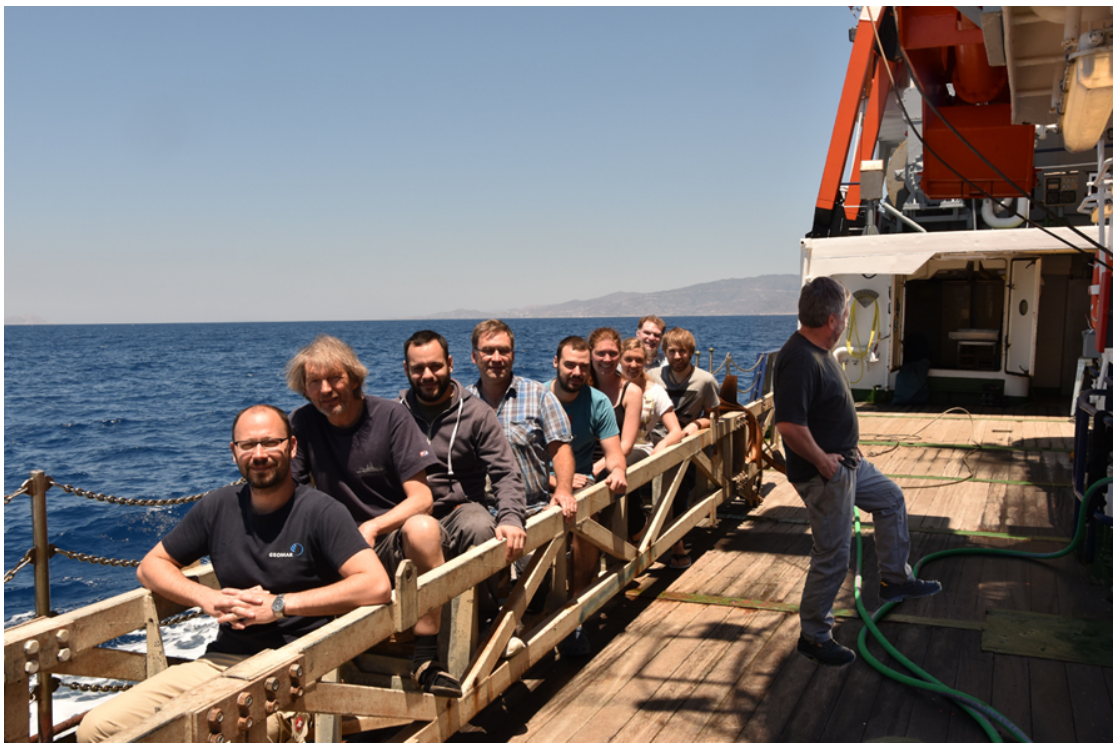

POS 513 scientific party – from left to right: Nico Augustin, Armin Freundt, Symeon Nasras, Thor Hansteen, Boris Karatsolis, Carina Sievers, Jenny Brandstätter, Steffen Kutterolf, Kai Fockenberg and Thorsten Schott.

1. Acknowledgements

We are very grateful to Captain Helge Volland and his officers and crew for their friendly hospitality and very efficient professional support which was essential to make this a successful expedition. We also acknowledge the Greek authorities for permission to work in their waters, as well as the German foreign ministry and embassy for their assistance. We are particularly grateful to Prof. Paraskevi Nomikou of University of Athens for all the relentless efforts she undertook to make this cruise possible.

2. Introduction

The Hellenic arc hosts several active volcanic systems of which the Santorini volcanic field and the Kos-Yali-Nisyros volcanic complex present particularly high threats due to recent unrest (2011-2012 and 1997-1998, respectively). Both systems have repeatedly produced highly explosive eruptions (VEI 4 to 7) during the last 160 kyrs and into historic times. The past record not only of the number of events but also of their magnitudes and intensities, which are inferred from tephra dispersal characteristics, is essential to predict future volcanic hazards and risks. This cruise complements earlier work on distal east-Mediterranean sediment cores, which captured the largest eruptions, by collecting cores at medial to proximal ranges in order to also record medium-size eruptions. The past highly explosive eruptions ranged from submarine through emergent to subaerial and the interaction with the sea increased the hazards (e.g., higher explosivity, tsunamis). One aim of this cruise is to sample tephra profiles in order to study vertical and lateral facies changes that will help to understand the nature of the interaction processes. Particularly useful is the opportunity to directly compare the products of submarine to subaerial eruptions emplaced in the same environment. The Hellenic arc is also a tectonically very active region. Our cruise complements earlier bathymetric maps by multibeam mapping of selected fault systems.

3. Background

Below the Aegean Sea, the eastern Mediterranean lithosphere (front part of the African plate) subducts with a velocity of ~4 cm/yr under the continental Aegean microplate, making the southern Aegean one of the most tectonically active regions of western Eurasia (e.g. McKenzie, 1972; Papazachos et al., 2005). Beginning in the Miocene (and continuing today, Zhu et al., 2006), slab retreat and rapid southward migration of the Crete trench led to widespread extension in the southern and central Aegean region causing a remarkable crustal thinning, as manifested by shallow Moho depth (~25 km beneath Santorini; Makris, 1977), deep basins (e.g. the Cretan basin) and seismically active faults and graben structures on the Aegean seafloor. The volcanic structures are hosted within extensional neotectonic basins/grabens crosscutting the Plio-Quaternary sedimentary sequences. The Aegean arc stretches from the Gulf of Saronikos in the northwest to an area close to the Anatolian coast in the East and includes the active volcanic centers at Methana, Milos, Santorini, and Nisyros (Fig. 1). Whereas large, composite volcanoes with caldera structures (Santorini and Kos-Yali-Nisyros) can be found in the central and eastern sectors of the arc, small, often monogenetic eruptive centers prevail in the western sector (Francalanci et al., 2005).

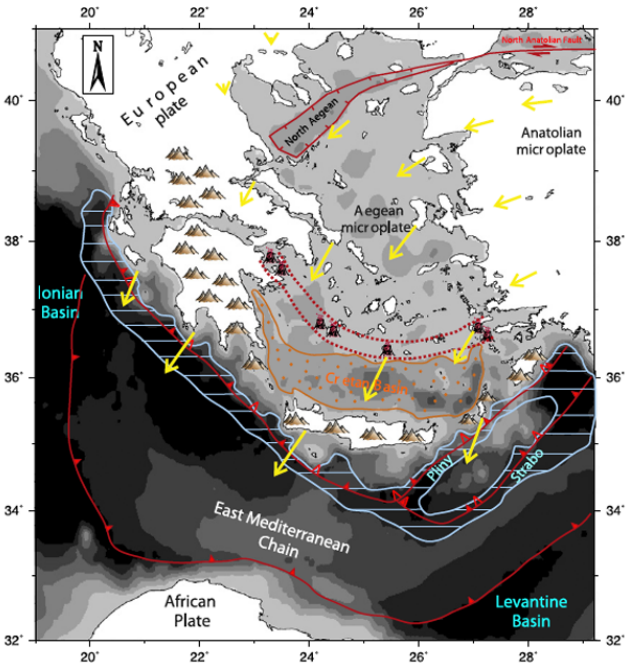

Fig. 1: Geodynamic structure of the Hellenic arc. The African plate subducts along the trench (red) generating (south to north) the Peloponnese-Crete island arc, the Cretan back-arc basin (orange) and the Aegean active volcanic arc. Yellow arrows are GPS vectors (ca. 4 cm/yr). From Nomikou et al. (2013c).

Santorini

The Santorini island group consists of the older islands Thira, Thirasia and Aspronisi that are arranged in a dissected ring around a flooded caldera. The caldera, a composite structure resulting from several collapse events, contains in its center the post-caldera volcanic islands Palea Kameni and Nea Kameni (Pyle and Elliott, 2006; Nomikou et al., 2014b). The oldest dated volcanic rocks are submarine tuffs, outcropping near Akrotiri in SW Thira, which yield early Quaternary ages and are speculated to originate from both Christiana and Akrotiri centers (Francalanci et al., 2005). Subaerial volcanism on Thira began about 650 ka ago (Druitt et al., 1999; Druitt, 2014), and continued until the present day. More than hundred explosive volcanic eruptions within the last 400.000 years, triggering at least four caldera collapses, make Santorini to one of the world's most violent volcanoes (Druitt and Francaviglia, 1992). The succession of the major tephras representing the most violent, paroxysmal eruptions is summarized in figure 2, and has been interpreted to represent two cycles of increasing eruption intensities and magnitudes (Druitt et al., 1989). Traces of these tephras can be expected widely distributed across the surrounding seafloor. However, in between numerous tephras from inter-Plinian activity occur (Vespa et al., 2006), some of which also emplaced marine ash beds (Satow et al., 2015). Parks et al. (2012) and Degruyter et al. (2015) show that magmatic evolution at Santorini is largely controlled by episodic melt replenishments from depth.

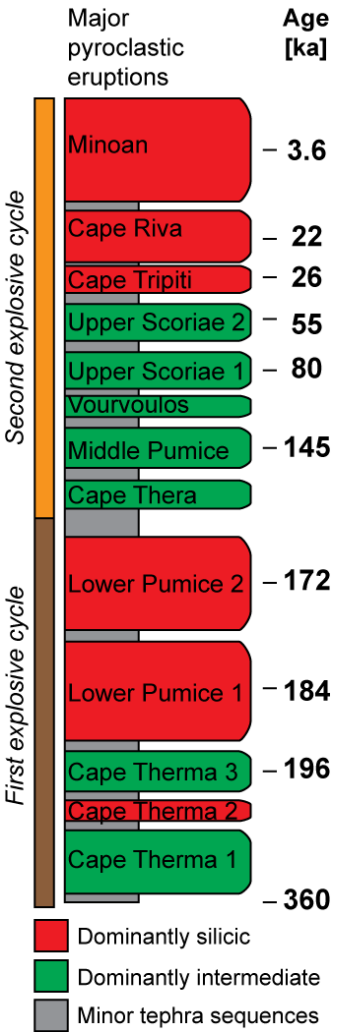

Fig. 2: Santorini stratigraphy of major tephras. From Druitt et al. (2015).

The last caldera collapse was caused by the late Bronze Age (3.6 ka) Minoan eruption (Druitt, 2014), which discharged about 80 km^3 DRE (Johnston et al., 2014) of rhyodacitic magma, distributed ash over a large area of the eastern Mediterranean and Turkey and led to (or significantly contributed to) the downfall of the advanced Minoan civilization (e.g., McCoy and Heiken, 2000; Vougioukalakis and Fytikas, 2005). After the Minoan eruption, volcanic activity continued mainly in the intra-caldera area where effusive and slightly explosive activity built up the Palea and Nea Kameni islands between 197 BC and 1950 AD (Nomikou et al., 2014b).

Kolumbo

Outside the Santorini caldera, about 7 km off the north-eastern coast of Thera, the ~350 m high submarine Kolumbo volcano and 19 other submarine cones formed within the fault-bordered Anhydros basin (Nomikou et al., 2012, 2013a). Seismic profiles across Kolumbo reveal a complex internal structure probably due to repeated phases of construction and destruction (Hübscher et al., 2015). In 1650 AD the Kolumbo volcano exploded in a paroxysmal event which ejected huge quantities of volcanic ash, caused a caldera collapse (Fig. 3), and generated a devastating tsunami (Nomikou et al., 2014a). This was the most hazardous and powerful eruption in the Greek territory in historic times killing more than 70 people on Thera and causing damages within a 150 km radius (Vougiokalakis and Fytikas, 2005). The submarine to emergent pumice deposits are about 250 m thick at the crater walls while distal fallout is found as far away as on the Turkish mainland. The stratigraphy of the proximal deposits, the eruptive mechanisms involved, and the pre-eruptive storage conditions of the rhyolitic magma have been investigated by Cantner et al. (2014). Fallout from this eruption forms the youngest widespread ash layer in the marine cores. The eruption model (Fig. 3) of Cantner et al. (2014) is based on the crater-rim deposits that were studied by submersible ROV. Fuller (2015) analyzed box and gravity cores collected around Kolumbo which all show fine-grained ash deposits in strong contrast to the fines-depleted breccias at the crater. Today, the shallowest point of Kolumbo volcano lurks only 18 m below sea level and there is continuing CO_2 degassing and hydrothermal activity in the north-eastern part of the crater (Carey et al., 2013; Kilias et al., 2013).

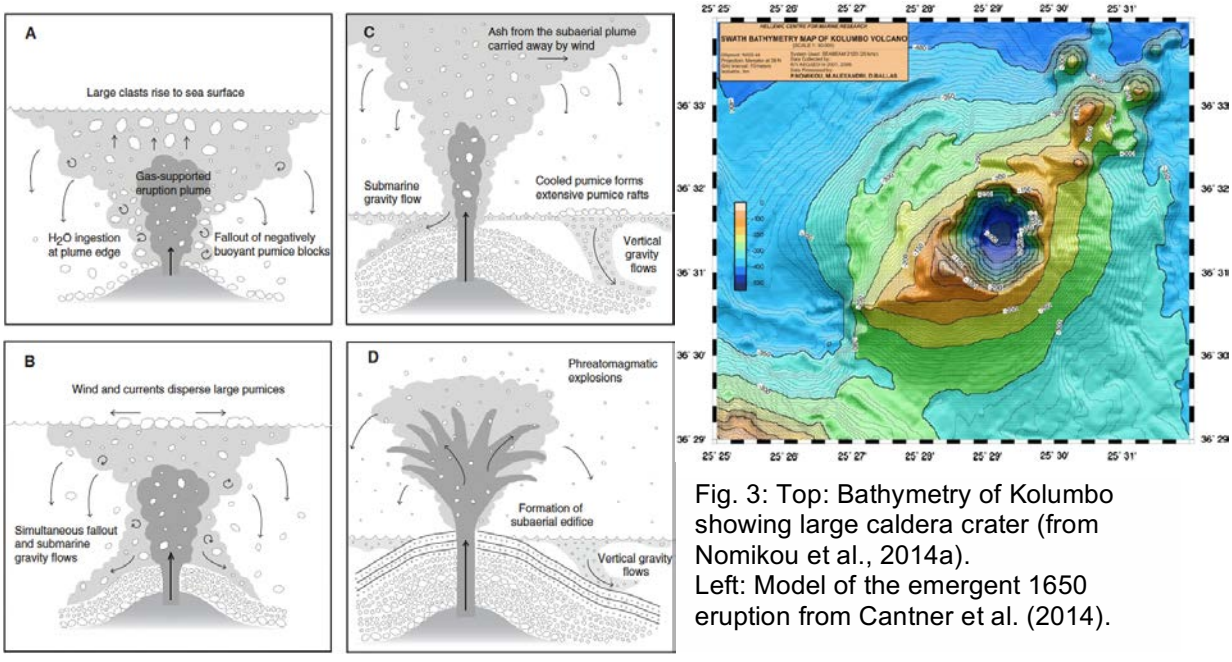

Fig. 3: Top: Bathymetry of Kolumbo showing large caldera crater (from Nomikou et al., 2014a).
Left: Model of the emergent 1650 eruption from Cantner et al. (2014).

Kos - Yali - Nisyros volcanic complex

The evolution of this volcanic complex probably reaches back to about 3 Ma. Of present interest is the evolution beginning with the paroxysmal eruption of the Kos Plateau Tuff (KPT) dated at 161 ka by Smith et al. (1996). This major phreatoplinian eruption (Allen and Cas, 1998) ejected an initial fallout but then discharged huge pyroclastic density currents that travelled over the sea (Allen and Cas, 2001) and emplaced thick ignimbrite on Kos and other islands up to 60 km away. The stratigraphy of the KPT has been studied in detail by Allen et al. (1999) and Allen (2001). About 60 km^3 DRE of rhyolite magma were erupted and are thought to have triggered subsidence of a submarine caldera basin south of Kos (Nomikou et al., 2013b) that was re-filled by younger volcanics. These younger volcanics include the Nisyros composite cone, the Yali pumice cone and lavas, and the Pleistocene to recent Strongyle basaltic andesite cone, all of which have been strongly affected by regional and possibly intra-caldera tectonic movements (Tibaldi et al., 2008b; Nomikou and Papanikolaou, 2011).

The stratigraphy of **Nisyros** is compiled in figure 4 from Di Paola (1974), Limburg and Varekamp (1991) and Francalanci et al. (1995). Due to limited outcrop on the small island, the internal stratigraphy of the Kyra pyroclastics is poorly known; the best record of these older deposits was obtained on the inner caldera walls (Volentik et al., 2002). Kuscu and Uslular (2014) report Kyra tephra in Turkey and emphasize the need for improved tephrostratigraphy to better constrain potential hazards. The major rhyolitic pumice deposits are the Lower Nisyros Pumice (LNP) and the Upper Nisyros Pumice (UNP), where eruption of the latter induced the caldera collapse (Fig. 4). The Nisyros caldera is covered by the Yali-2 pumice fallout and partly filled by lavas and domes.

A major problem in understanding the evolution of Nisyros are the contradicting age constraints as exemplarily illustrated in figure 5. Due to these age conflicts, the age of a major sector collapse on Nisyros could not yet be well constrained (Tibaldi et al., 2008a; Livanos et al., 2013) and time series to be used in volcanic hazard assessment remain highly uncertain (e.g., St. Seymour and Vlassopoulos, 1989; Kinvig et al., 2010). Marine tephra successions from around Nisyros may help to clarify these conflicts.

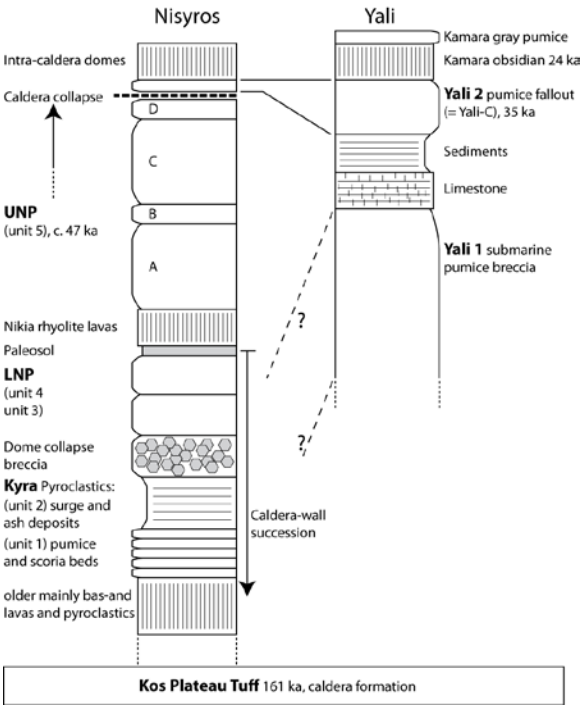

Left Fig. 4: Composite stratigraphic profiles of Nisyros and Yali. Compiled from Limburg and Varekamp (1991), Francalanci et al. (1995), Allen and McPhie (2000).

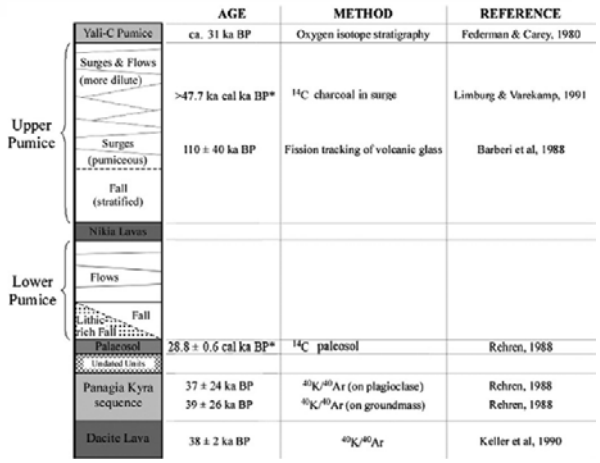

Top Fig. 5: Conflicting age data for Nisyros rock units. From Tomlinson et al. (2012b).

The volcanic succession at **Yali** comprises a >150 m thick submarine pumice breccia (Yali 1, Fig. 4) covered by an about 2 m thick package of limestone and bioclastic sandstone representing the emergent phase of island tectonic uplift (Allen and McPhie, 2000). This is overlain by the Yali-2 subaerial pumice fallout which is post-dated by the 24 ka Kamara obsidian lava which is overlain by a gray pumice fallout with perlitic clasts (Fig. 4). The Yali-2 pumice has been dated at about 35 ka but the age of Yali-1 is unknown. Pyle and Margari (2009) argue that Yali-1 would be older than the Lower Pumice of Nisyros. Allen and McPhie (2000) have logged and analyzed the Yali-1 pumice breccia in great detail and derived a model for the submarine eruption, fragmentation and emplacement processes.

Marine tephrostratigraphy

The eastern Mediterranean and Aegean seas have long been a target for sediment coring projects (Fig. 6) which have resulted in a fairly well established grid of major, widely dispersed marker tephras (e.g., Keller et al., 1978; Federman and Carey, 1980). Supporting evidence came from lake sediment cores (e.g., Margari et al., 2007) or from sediments preserved in caves (e.g., Karkanas et al., 2015). The ashes found in this region derive from Aegean volcanoes but also from Italian volcanoes and those in Central Turkey.

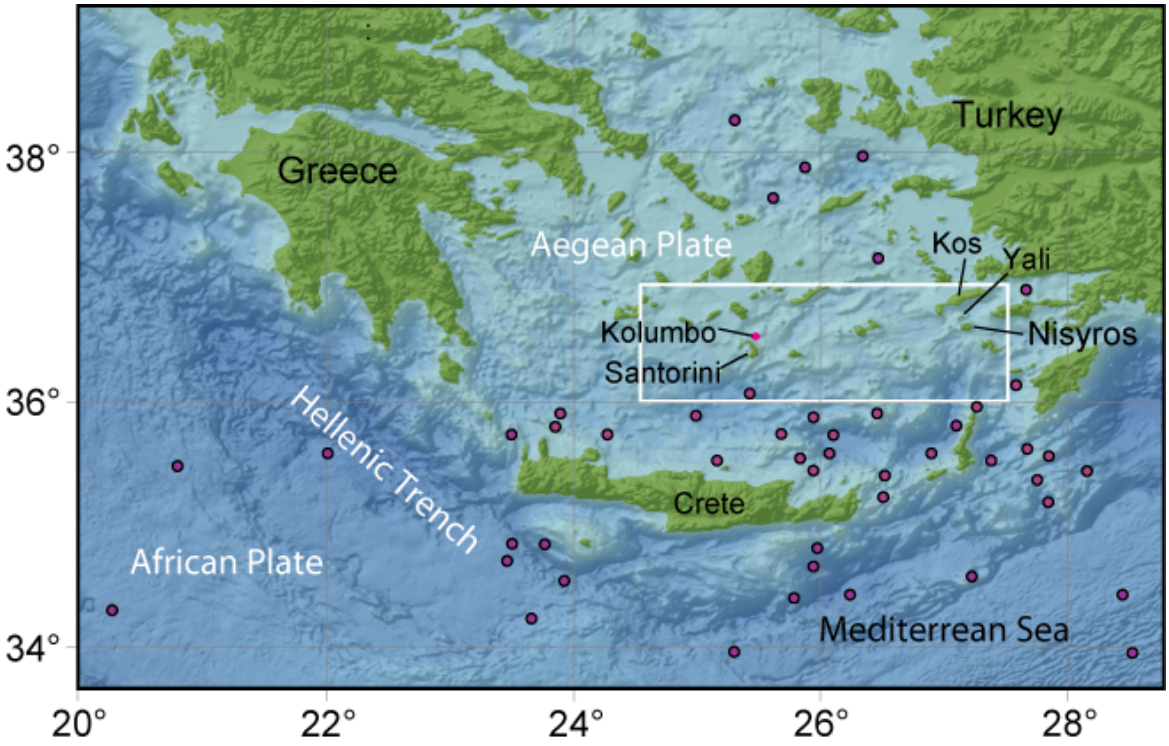

Fig. 6: Map of the Aegean Sea showing positions of marine sediment cores from previous projects. White box outlines the work area for this proposal (see Fig. 10) which complements previous sediment coring (Keller et al., 1978; Federman & Carey, 1980; Vinci, 1985; Hardiman, 1999; Aksu et al., 2008). Bathymetry from www.geomapapp.org

Particularly major Italian tephras are widely dispersed across the Aegean due to the preferential higher altitude winds towards the ENE. Fortunately, these different source regions can be distinguished geochemically. The alkaline and peralkaline Italian volcanics differ from the calc-alkaline rocks of the Aegean arc already in major element (bulk-rock

and glass) compositions (e.g., Clift and Blusztajn, 1999). For further discriminations, in part also between individual tephras from one source region, there now exists an extensive data base that is particularly detailed for the Italian volcanic systems (Tomlinson et al., 2012a, 2015; Wulf et al., 2004, 2008, 2012) but also covers Quaternary tephras from other European regions including the Aegean Sea (Bronk Ramsey et al., 2015a, b; Satow et al., 2015).

The Mediterranean marine sediment records have been subdivided into foraminifer zones V through Z, and the ashes in these zones have been named Z-2, Y-5, W-3 and so on. Some widespread tephras had been identified early on (Keller et al., 1978; Federman and Carey, 1980; Vinci, 1985) such as the Minoan Tephra as Z-2, Cape Riva (Akrotiri) Tephra as Y-2, the Yali-C (Yali-2) pumice in the Y zone, the Campanian Ignimbrite as Y-5, and the Kos Plateau Tuff as W-3 (Fig. 7). The increasing availability of trace-element microanalyses has led to a large number of additional identifications and corrections of correlations over the past decade while sediment coring also progressed from the eastern Mediterranean northward across the Aegean Sea up to the Marmara Sea (Wulf et al., 2002; Margari et al., 2007; Aksu et al., 2008). Moreover, cryptotephras (macroscopically non-visible ash layers) have been recognized in addition to distinct visible ash beds (e.g., Satow et al., 2015; Çağatay et al., 2015). Consequently, a number of additional tephras could be recognized in the marine sediments such as the Pantelleria Green Tuff as Y-6 or tephras from central Turkey as Z-3 to Z-5 (Margari et al., 2007; Karkanas et al., 2015) and a Campi Flegrei tephra as Y-3 (Albert et al., 2015). At the same time, a number of contradictions and uncertainties still remain to be resolved. For example, Hardiman (1999) claimed to have found the Nisyros Lower Pumice at 35 ka in a core 75 km SW of the island but that the Upper Pumice would not occur. Tomlinson et al. (2012b), in contrast, find that all Nisyros ash in marine cores is Upper Pumice and that Lower Pumice does not occur. Vinci (1985) and Narcisi and Vezzoli (1999) place Nisyros ash between Y-2 and Y-3 in the east Mediterranean but further north in the Aegean Sea Nisyros ash occurs below Y-5 (Aksu et al., 2008; Satow et al., 2015). As another example, Narcisi and Vezzoli (1999) placed Yali-C above Y-4 (cf. Fig. 7) where it was dated at 31 ka (Tomlinson et al., 2012b) while Satow et al. (2015) found Yali-C below Y-4 at 35 ka. The fact that these uncertainties exist particularly for the Nisyros-Yali system is partly due to the similarity in the compositions of

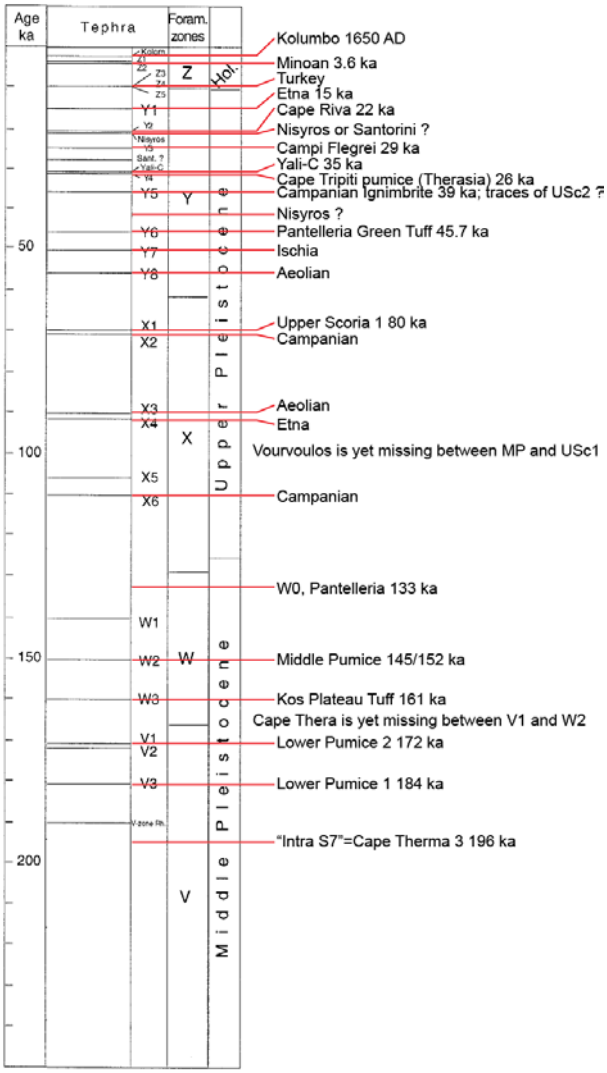

Fig. 7: Composite stratigraphic column of central to east Mediterranean marine sediment cores. Modified from Narcisi and Vezzoli (1999) and complemented by more recent identifications of major tephras (red lines) as discussed in the text.

these rhyolites but probably it is also due to the circumstance that no sediment cores yet exist in the vicinity of these islands, the closest core position is 60 km away (Fig. 6).

4. Cruise Narrative

4.1 Daily Narrative

(see station list 4.2 and station map 4.3 below)
May 9: At 9:00 the ship left Heraklion harbor and reached the first work station in the afternoon but then wind and swell were too strong for deployment of the gravity corer. Nighttime mapping of fault NW of Santorini could, however, be performed (station 1).
May 10: Stations 2 to 5
We began the coring campaign along a track leading from the north of Santorini to the south of Milos. However, we soon learned about the difficulties of being limited to work only close to land within the 6 nm zone, where coarse-grained sediment, cemented coral debris and similar materials on the seafloor prohibited the extraction of proper cores despite repeated attempts, either due to no or insufficient penetration or to loss of corse-grained sediment during heaving. Therefore we equipped the gravity corer with a trigger system as described in section 6. The night shift mapped a fault system south of Milos (station 6).
May 11: Stations 7-1 to 8-2
The first 2 m core proved the value of the modified corer, and south of Milos we then recovered a 7.5 m core. The night transit took us back close to Santorini.
May 12: Stations 9 to 12
West of Christiana we recovered a 3.4 m core with 2 ash beds. Three stations along a line from S to E of Santorini remained unsuccessful despite the corer setup, the trouble again being too coarse sediment on the seafloor. Overnight mapping showed an interesting system of cross-cutting faults SE of Ios (station 13).
May 13: Stations 14 to 17-2
Further to the east we gained 4 m and 5 m long cores but subsequent stations in shallower waters gave short cores only. Station 18 was mapping near Amorgos island.
May 14: Stations 19 to 22
The region 10 to 20 km Se and E of Columbo volcano yielded successful cores containing stratified lapilli and ash of the 1650 eruption. In an attempt to recover undisturbed near-surface sediment we mounted the giant box corer to cover an eastern semicircle around Santorini. The 20 cm and 40 cm thick profiles with thin ash horizons we recovered were, however, insufficient to penetrate the Columbo ash. Mapping south of Anafi island was station 23.
May 15: Stations 24 to 28
After another trial, we terminated the box corer deployments and returned to gravity coring. However, within 10-20 km distance east of Santorini, recovered cores did not exceed 80 cm length. Further east, beyond the island of Anafi, however, recovery increased to around 3 m at two stations. At night the mapping near Anafi was continued (station 29).
May 16: Stations 30-1 to 32
Along three stations to the north of Astipalea all cores reached 4 to 5 m length. Mapping to the west of that island followed at night (station 33).
May 17: Stations 34 to 37
Turning southeastward along three stations gave 3.5 to 4.5 m long cores. Particularly interesting was the repeated occurrence of a mafic ash bed that we had found the first time on May 15. Station 38 was the mapping of fault structures north of Karavi islet.
May 18: Stations 39 to 41
60 km further south, near the north rim of the deep basin northeast of Crete, we succeeded in pulling three 5-6 m long cores with the 10 m corer tube. Details of the Syrna fault zone were mapped at night as station 42.
May 19: Stations 43 to 46

Continued use of the 10 m tube yielded 3.2 to 6.5 m long cores at the four stations between Syrna and Nisyros, containing a pumice lapilli layer possibly equivalent to the Upper Nisyros Pumice. A rather unusual find was a layer a fine-ash layer stuffed full with accretionary lapilli. Station 47 extended the mapping at Syrna.

May 20: Stations 48 to 50

Strong winds and swell did not allow us to continue mapping over night and we also skipped the first two stations in the morning. At noon the EUA observer disembarked to a shuttle boat that took him to Kos; his early leave had required intense communications with several administrations in order to get the permissions for his departure as well as to continue our work without him. The afternoon with improved weather conditions in the shadow of Kos north of Nisyros rewarded us with a 3.8 m core containing numerous thin ash beds, probably the traces of smaller post-caldera eruptions on Nisyros. In the second core, east of Nisyros, these were largely absent. We returned to one of the stations missed in the morning and recovered a 4.2 m core with several ash and fine pumice lapilli horizons and an impressive >60 cm thick pumice lapilli deposit at the base, which probably is the 47 ka Upper Nisyros Pumice from the caldera-forming eruption.

May 21: Stations 51 to 54

We completed the circle around Nisyros-Yali. The four cores with 2.3 to 5.6 m recovery contained several pumice-bearing ash layers which we tentatively relate to Nisyros eruptions. Overnight we returned to the region northwest of Santorini.

May 22: Stations 55 to 58-2

We re-tried coring with the trigger setup in the region where we had failed with the simple gravity corer in the beginning. At night we extended the mapped region south of Sikinos (station 59).

May 23: Stations 60 and 61

In total, these 1.5 days of 6 re-trials only yielded 2 significant core recoveries.

The afternoon was used to clean the ship and pack up while simultaneously further extending the mapping near Sikinos (station 62). During the night we sailed back to Crete and entered Heraklion harbor at 8:00 the next morning.

May 24: The heavy equipment was unloaded into a GEOMAR owned container. Unfortunately, however, the second, rented container had not been delivered. Therefore unloading of the cores and other boxed materials was delayed by two days.

4.2 Station List

GC= gravity corer
GCs= GC with trigger
-3 = 3 m tube
-5 = 5 m tube
-10 = 10 m tube

BC= box corer
Map= bathymetric mappings

Stationlist POS 513

Time UTC = ship time -3h

Station	Date	Water Depth	Instrument	Station coordinates			max. Tension	Penetration	Recovery
				Time UTC	*Latitude (NS)*	*Longitude (EW*	kN	m	m
1			Map 1	south of Sikinos island					
2-1	10.05.17	108	GC-5	04:16	36°35,223	25°15,981	15	1,5	0,52
2-2	10.05.17	107	GC-5	04:56	36°35,212	25°15,971	?	?	?
3-1	10.05.17	329	GC-5	07:25	36°32,424	25°05,391	17,6	2,5	ø
3-2	10.05.17	330	GC-5	08:02	36°32,424	25°05,391	17,2	2,5	ø
4-1	10.05.17	526	GC-5	09:32	36°30,202	24°55,836	20,3	0,2	ø
4-2	10.05.17	525	GC-5	10:11	36°30,217	24°55,847	20,7	ø	ø
5	10.05.17	525	GCs-5	12:11	36°35,166	24°46,113	31	1,5	0,65
6			Map 2	south of Milos island					
7-1	11.05.17	267	GCs-3	05:36	36°34,354	24°30,120	36	3	2,04
7-2	11.05.17	268	GC-3	07:11	36°34,349	24°30,107	20,7	0,6	0,44
8-1	11.05.17	964	GCs-3	09:53	36°28,325	24°14,091	72	5	3
8-2	11.05.17	964	GCs-10	12:20	36°28,355	24°14,104	82	10,6	7,44
9	12.05.17	560	GCs-5	05:07	36°15,997	25°05,152	52	4,8	3,38
10	12.05.17	458	GCs-5	08:25	36°15,280	25°27,617	35	ø	ø
11	12.05.17	475	GCs-5	10:42	36°21,564	25°37,307	32	ø	ø
12	12.05.17	612	GCs-5	13:09	36°28,810	25°46,384	35,4	2,5	0,4
13			Map 3	southeast of Ios island					
14	13.05.17	583	GCs-5	05:15	36°40,668	25°50,789	60	5,2	4
15	13.05.17	450	GCs-5	07:31	36°42,540	25°43,094	65,8	5,5	4,85
16-1	13.05.17	466	GCs-5	09:34	36°37,680	25°34,964	41	2,5	0,4
16-2	13.05.17	465	GCs-5	10:30	36°37,749	25°34,916	47	2	0,8
17-1	13.05.17	282	GCs-5	12:21	36°37,237	25°26,997	31	1,2	0,6
17-2	13.05.17	412	GCs-3	13:30	36°35,849	25°26,432	24	1	ø
18			Map 4	southwest of Amorgos island					
19	14.05.17	408	GCs-3	05:20	36°26,506	25°34,429	27,4	1,5	0,68
20	14.05.17	280	GCs-3	07:10	36°33,345	25°39,825	56	3,2	2,01
21	14.05.17	452	BC	09:41	36°42,552	25°43,076	13,7	0,2	0,2
22	14.05.17	583	BC	11:34	36°40,675	25°50,778	18,4	0,46	0,46
23			Map 5	south of Anafi island					
24	15.05.17	335	BC	05:20	36°20,455	25°38,492	12	0,5	9,3
25	15.05.17	397	GCs-3	06:34	36°20,717	25°38,285	43	1,2	0,6
26	15.05.17	614	GCs-3	08:35	36°28,771	25°46,363	45,8	2,5	0,85
27	15.05.17	163	GCs-3	11:29	36°15,245	26°00,324	39,8	3,1	2,85
28	15.05.17	415	GCs-5	14:16	36°31,892	26°01,037	60	4,5	3,13
29			Map 5	continued					
30-1	16.05.17	421	GCs-5	05:17	36°23,668	25°57,809	66,7	5,2	2,2
30-2	16.05.17	421	GCs-5	06:12	36°23,670	25°57,823	56	4,8	4,4
31	16.05.17	436	GCs-5	09:41	36°38,209	26°10,492	74	5,5	4,45
32	16.05.17	606	GCs-5	12:21	36°50,349	26°15,377	77,7	6	4,66
33			Map 6	west of Astipalea island					
34	17.05.17	493	GCs-5	05:04	36°42,102	26°29,068	76,2	5,3	4,61
35	17.05.17	464	GCs-5	07:15	36°33,325	26°35,133	66,3	4,9	4,26
36	17.05.17	475	GCs-5	09:37	36°26,462	26°27,281	63,4	4	3,28
37	17.05.17	500	GCs-5	11:35	36°25,176	26°15,985	53	5,5	4,26
38			Map 7	north of Karavi islet					
39-1	18.05.17	822	GCs-5	02:59	36°05,008	26°31,028	79,8	7	ø
39-2	18.05.17	820	GCs-10	05:40	36°04,997	26°31,024	70	9	5,85
40	18.05.17	747	GCs-10	09:02	35°51,478	26°19,795	70,9	7,5	5
41	18.05.17	1264	GCs-10	13:04	35°59,700	26°47,365	68	7,5	5
42			Map 8	around Syrna island					
43	19.05.17	526	GCs-10	05:16	36°27,895	26°43,690	79	5,5	4,3
44	19.05.17	529	GCs-10	07:08	36°31,548	26°53,260	100	7	5,17
45	19.05.17	672	GCs-10	09:30	36°26,811	27°01,057	68	9	6,46
46	19.05.17	353	GCs-10	11:57	36°23,059	26°49,641	47	4,5	3,1
47			Map 8	continued					
48	20.05.17	630	GCs-5	09:38	36°45,302	27°11,505	64,7	5,5	3,8
49	20.05.17	537	GCs-5	11:30	36°40,710	27°13,539	50,1	6,5	3,62
50	20.05.17	475	GCs-5	13:39	36°40,056	27°02,229	48	5,3	4,35
51	21.05.17	302	GCs-5	05:00	36°36,914	27°16,056	72,9	2,5	2,3
52	21.05.17	372	GCs-5	06:32	36°32,756	27°18,273	43,5	3,1	2,89
53	21.05.17	684	GCs-10	09:02	36°28,606	27°03,751	74,2	7	5,59
54	21.05.17	406	GCs-10	13:06	36°12,000	26°42,481	47	3	2,47
55	22.05.17	525	GCs-5	03:24	36°30,199	24°55,834	49,2	1,5	0,89
56	22.05.17	274	GCs-5	06:33	36°45,891	25°02,170	61,6	6,8	5,27
57	22.05.17	400	GCs-5	10:00	36°33,664	25°25,128	23,1	ø	ø
58-1	22.05.17	451	GCs-5	12:06	36°38,054	25°33,102	36,7	ø	ø
58-2	22,05.17	457	GCs-5	13:05	36°38,585	25°33,126	36,9	1	0,27
59			Map 1	continued					
60	23.05.17	474	GCs-5	05:15	36°20,126	25°11,051	30	ø	0,21
61	23.05.17	525	GCs-5	06:48	16°15,129	25°16,234	29	ø	0,38
62			Map 1	continued					

4.3 Map of stations

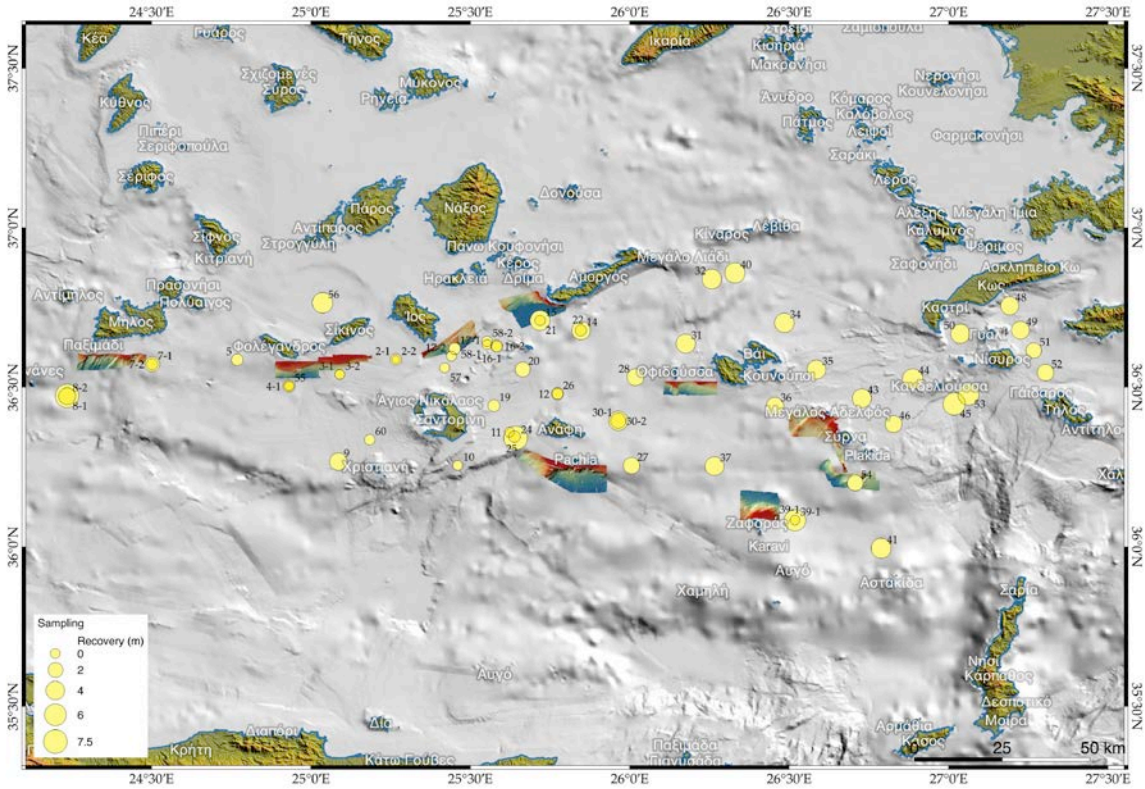

Fig. 8: Map of stations in which the yellow dots for sediment corings are scaled to the recovered core length. Station numbers refer to 4.2. Colored fields are the bathymetrically mapped areas.

5. Bathymetry *(N. Augustin, S. Nasras)*

During RV Poseidon cruise POS513 multibeam mapping was carried out by a Seabeam 3000 series echosounder system (SB3100) provided by ELAC Nautik GmbH. The SeaBeam 3100 multibeam echosounder (MBES) collects bathymetric, corrected backscatter, side scan and water column imaging (WCI) data at medium depths. The configuration installed on RV Poseidon operates in the 50 kHz frequency band at water depths ranging from 3 m below the transducers to approximately 3,000 m. However, beside this theoretical value we observed that the best operation depth under optimal weather conditions is between >100 m to <2000 m water depth. It has an across-ship swath width of up to 140 degrees with up to 630 beams for each multi-ping. The complete system consists of 2 transmitter/ receiver units, a motion sensor (Coda Octopus F180), and a salinometer installed on RV Poseidon. The system was operated with HydroStar v4.0. Data acquisition was performed with Hypack 2016. The Hysweep survey module of Hypack bundle collected all data from the SeaBeam echo sounder in HSX data format which was used for further processing. Since the HSX data contain all necessary information for post processing work the native ELAC XSE-data format was not stored during the cruise.

For sound velocity corrections, a CTD profile, obtained during cruise POS511 was used. The recorded HSX raw data were copied and (preliminary) post processing was done with QPS Qimera (Version 1.5.1, Mac). Maps were created in QGIS 2.18. Preliminary grids yielded a spatial resolution of 15-20 m in water depths of up to 900 m. However, final data processing and gridding will be done after the expedition at GEOMAR, Kiel and the University of Athens. The data will be also stored at GEOMAR, Kiel for scientific use and

become public available via the Pangaea scientific data repository (pangaea.de) at a later stage

Multibeam mapping was limited to the 6 nm buffer zone of the Aegean islands and served to add bathymetric data to existing datasets of the Southern Agean sea. Therefore 9 mapping areas (Fig. 8) scatter between the islands of Milos, the most western target area, and Astypalaia in the east. Main mapped seafloor features were tectonic lineaments as e.g., south of Milos and parts of the Ios and Amorgos fault zones. Erosion structures were mapped e.g. at the island footwalls south of Anafi and SE of Astypalaia (see also examples in Figures 9 – 11).

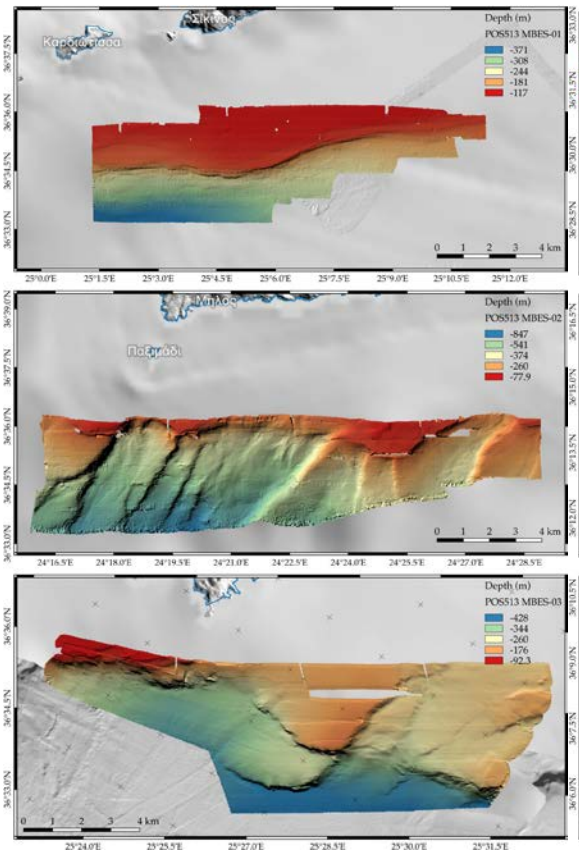

Fig. 9: Bathymetrc maps of preliminary postprocessed data showing tectonic lineaments south of Sikinos (upper), Milos (middle) and Ios island (lower).

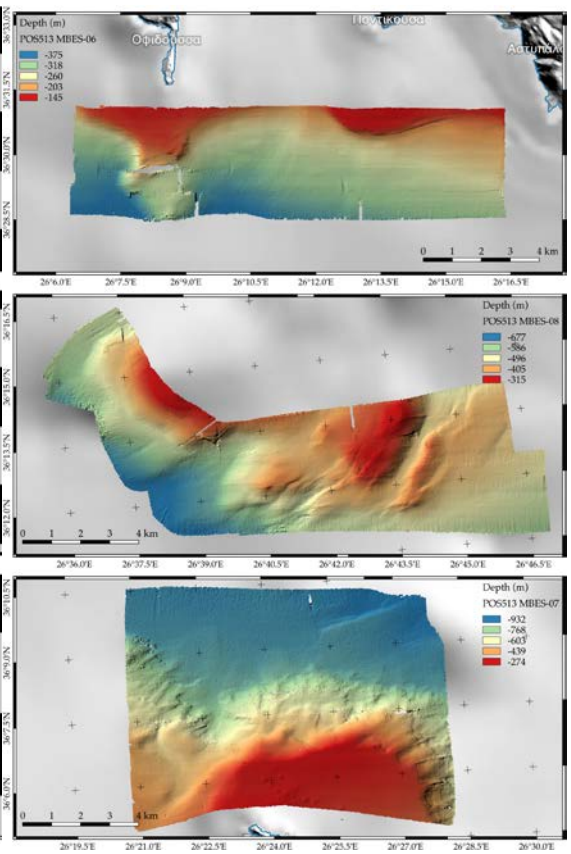

Fig. 10: Bathymetrc maps of preliminary postprocessed data showing the footwall morphology south of Astypalaia (upper), some bended tectonic lineaments south of Syrna island (middle) and erosion of the northern base of Zaphora island (lower).

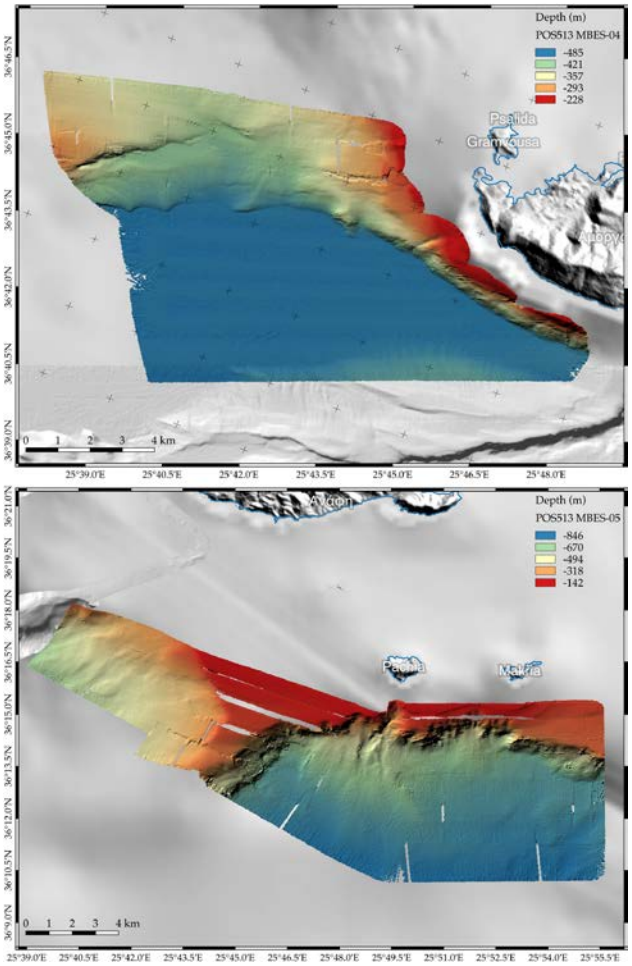

Fig. 11: Bathymetrc maps of preliminary postprocessed data showing tectonic lineaments east of Amorgos (upper), and footwall erosion at the Pacha and Makra islands, south of Anafi island (lower).

6. Gravity Corer Setup

The first work day showed that deployment of the gravity corer in its standard setup (2-tonnes weights above a 3/5/10 m long steel tube) was not efficient to recover significant core lengths. A likely reason was the impact of the corer on the seafloor which was limited by the max. 1.5 m/s winch speed. We therefore equipped the corer with a trigger mechanism that realeased the corer into free fall over the final 3 m to the seafloor, thus generating much higher impact speeds (Fig. 12). The trigger was kept locked by a leading weight and was released when that weight hit the seafloor. Setting up the corer for slacking off, and retrieving it after heaving up, required more efforts by the deck crew but that was worth while since we obtained much more successful core recoveries with this method.

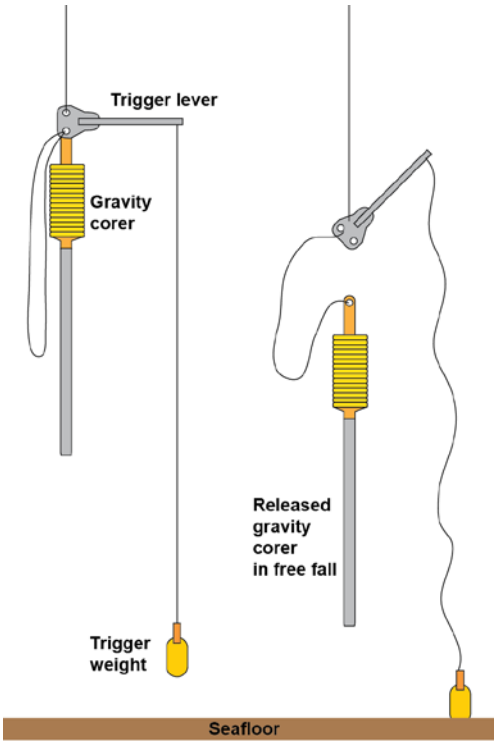

Fig. 12: Schematic illustration of gravity corer release triggering.

7. Sediment Core Profiles

47 out of 57 gravity corer deployments yielded sediment cores from 21 to 744 cm length, providing us with a total of 139 m sediment core. 32 cores are longer than 2 m and should extend well into the Pleistocene. All cores were immediately cut open on board, stratigraphically logged and photographed, and ash beds or ash pods were sampled. Small sub-samples were used to produce smear slides for microscopical inspection. These observations allowed us to make some preliminary correlations with major tephras known from land. However, these correlations as well as the origin of numerous yet unknown tephras need to be further investigated by geochemical analyses.
As an example, Figure 13 shows the core from station 8-2 south of Milos which contains 8 well developed ash beds. Numbers 1 and 2 are the Kolumbo and Minoan tephras, respectively. Numbers 4-6 are most likely felsic tephras from Santorini that still need to be correlated with the stratigraphy on land. Ash beds 7 and 8 are mafic tephras of yet unknown origin. In the central region of the island arc, the only 400 years old Kolumbo tephra is typically covered by about 30 cm sediment; this indicates a surprisingly high sedimentation rate of about 75 cm/ky.

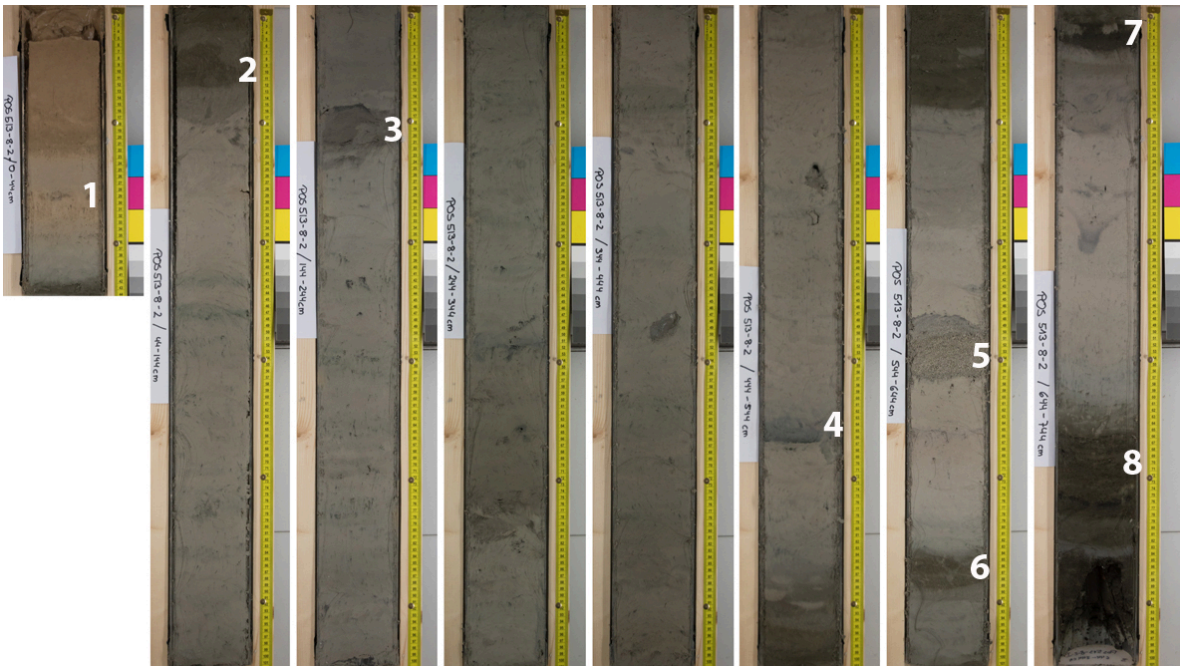

Fig. 13: Core photographs showing the stratigraphic succession at station 8-2 south of Milos (see Fig. 8). This was the westernmost sampling site of cruise POS 513.

At the eastern part of the island arc, we have also found tephras from the Kos-Yali-Nisyros volcanic complex. The best example is a pumice lapilli layer in core 45 (Fig. 8) at 3 m below seafloor (no. 3 in Fig. 14) that we correlate with the caldera-forming Upper Nisyros Pumice (UNP, Fig. 4) eruption 47 ka ago. If this correlation proves correct, the sedimentation rate in the eastern part of the island arc would be only about 7 cm/ky, i.e. about ten times lower than in the central part.
Particularly interesting is the occurrence not only of felsic but also of mafic widespread tephras. We have previously identified the occurrence of tephras from presumed “basaltic” Plinian eruptions at other settings (e.g., Central American subduction zone, Kutterolf et al 2008a, b; Cape Verdes, Eisele et al. 2015), and have now found evidence for such eruptions also at the Aegean islands. A prominent example is shown in Figure 14, where

we correlate a mafic fine lapilli layer at site 28 (no. 1) with a mafic ash layer at the same depth (presumably same age) at site 36 (no. 2). These sites lie about mid-way between Santorini and Nisyros, are 45 km apart, and the eastward decrease in thickness and grain size strongly suggests an origin at Santorini.

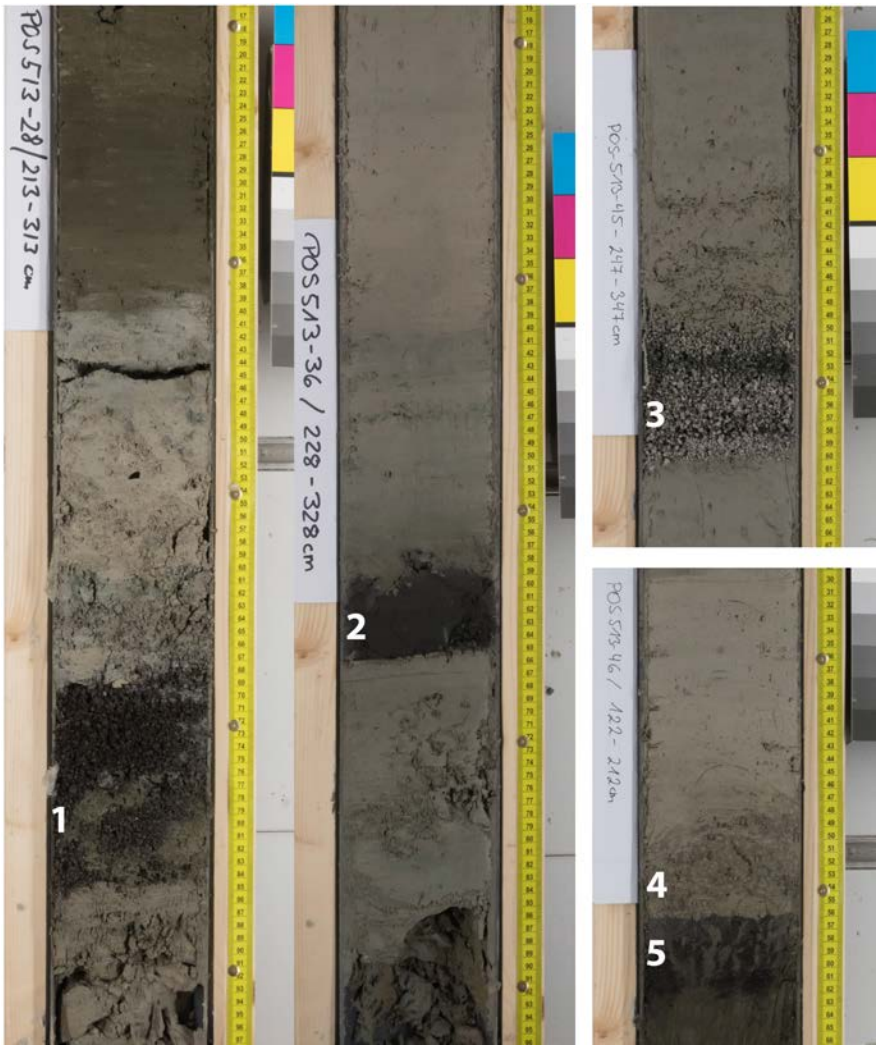

Fig. 14: Core photographs from sites 28 (left) and 36 (center) each showing a mafic tephra layer at about 3 m below seafloor (nos. 1, 2). No. 3 is a pumice lapilli layer in core 45 at 307 cm bsf which we tentatively correlate with the Upper Nisyros Pumice. No. 4 is an ash layer with abundant accrecionary lapilli at 178 cm bsf in core 46; it immediately overlies a mafic ash layer (no. 5). See Fig. 8 for site positions.

A somewhat surprising discovery was the occurrence in core 46 of an ash layer stuffed full with accretionary lapilli 3 to 5 mm in diameter, where it was emplaced in 350 m water depth. Intuitively one might expect that such loose ash aggregates would disaggregate during settling through the water column but obviously this was not the case. This ash bed (no. 4 in Fig. 14) immediately overlies a mafic fallout ash (no. 5), suggesting a genetic relation such as a magmatic eruption that turned phreatomagmatic in its course.

8. Final notes

Both work and archive halves of all cores have been stored in the cooled GEOMAR core repository and will be available for further sampling and studies. A subset of samples has already been sent to University of Athens for microfossil studies. The new bathymetric

data is available through the GEOMAR data storage, and has also been sent to Prof. Nomikou, University of Athens.

9. References

Aksu AE, Jenner G, Hiscott RN, Isler EB (2008) Occurrence, stratigraphy and geochemistry of Late Quaternary tephra layers in the Aegean Sea and the Marmara Sea. Marine Geology 252: 174-192

Albert PG, Hardiman M, Keller J, Tomlinson EL, Smith VC, Bourne AJ, Wulf S, Zanchetta G, Sulpizio R, Müller UC, Pross J, Ottolini L, Matthews IP, Blockley SPE, Menzies MA (2015) Revisiting the Y-3 tephrostratigraphic marker: a new diagnostic glass geochemistry, age estimate, and details on its climatostratigraphical context. Quat Sci Rev 118: 105-121

Allen SR (2001) Reconstruction of a major caldera-forming eruption from pyroclastic deposit characteristics: Kos Plateau Tuff, eastern Aegean Sea. J Volcanol Geotherm Res 105: 141-162

Allen SR, Cas RAF (1998) Rhyolitic fallout and pyroclastic density current deposits from a phreatoplinian eruption in the eastern Aegean Sea, Greece. J Volcanol Geotherm Res 86: 219-251

Allen SR, Cas RAF (2001) Transport of pyroclastic flows across the sea during the explosive, rhyolitic eruption of the Kos Plateau Tuff, Greece. Bull Volcanol 62: 441-456

Allen SR, McPhie J (2000) Water-settling and resedimentation of submarine rhyolitic pumice at Yali, eastern Aegean, Greece. J Volcanol Geotherm Res 95: 285-307

Allen SR, Stadlbauer E, Keller J (1999) Stratigraphy of the Kos Plateau Tuff: Product of a major Quaternary explosive rhyolitic eruption in the eastern Aegean, Greece. Int J Earth Sci 88: 132-156

Bronk Ramsey C, Albert PG, Blockley SPE, Hardiman M, Houley RA, Lane CS, Lee S, Matthews IP, Smith VC, Lowe JJ (2015a) Improved age estimates for key Late Quaternary European tephra horizons in the RESET lattice. Quat Sci Rev 118: 18-32

Bronk Ramsey C, Housley RA, Lane CS, Smith VC, Pollard AM (2015b) The RESET tephra database and associated analytical tools. Quat Sci Rev 118: 33-47

Çağatay MN, Wulf S, Sancar Ü, Özmaral A, Vidal L, Henry P, Appelt O, Gasperini L (2015) The tephra record from the Sea of Marmara for the last ca. 70 ka and its palaeoceanographic implications. Marine Geology 361: 96-110

Cantner K, Carey S, Nomikou P (2014) Integrated volcanologic and petrologic analysis of the 1650 AD eruption of Kolumbo submarine volcano, Greece. J Volcanol Geotherm Res 269: 28-43

Carey S, Nomikou P, Croff Bell K, Lilley M, Lupton J, Roman C, Stathopoulou E, Bejelou K, Ballard R (2013) CO2 degassing from hydrothermal vents at Kolumbo submarine volcano, Greece, and the accumulation of acidic crater water. Geology 41: 1035-1038

Clift PD, Blusztajn J (1999) The trace-element characteristics of Aegean and Aeolian volcanic arc marine tephra. J Volcanol Geotherm Res 92: 321-347

Degruyter W, Huber C, Bachmann O, Cooper KM, Kent AJR (2015) Magma reservoir response to transient recharge events: The case of Santorini volcano (Greece). Geology, doi:10.1130/G37333.1

DiPaola GM (1974) Volcanology and petrology of Nisyros Island (Dodecanese, Greece). Bull Volcanol 38: 944-987

Druitt TH (2014) New insights into the initiation and venting of the Bronze-Age eruption of Santorini (Greece), from component analysis. Bull Volcanol 76: 794, DOI 10.1007/s00445-014-0794-x

Druitt TH, Edwards L, Mellors RA, Pyle DM, Sparks RSJ, Lanphere M, Davies M, Barriero B (1999) Santorini volcano. Geol Soc London Mem 19: pp 165

Druitt TH, Francalanci L, Fabbro G (2015) Field guide to Santorini volcano. MeMoVolc short course, Santorini: pp. 56

Druitt TH, Francaviglia V (1992) Caldera formation on Santorini and the physiography of the islands in the late Bronze Age. Bull Volcanol 54: 484–493

Druitt TH, Mellors RA, Pyle DM, Sparks RSJ (1989) Explosive volcanism on Santorini, Greece. Geol Mag 126: 95-126

Eisele S, Reißig S, Freundt A, Kutterolf S, Nürnberg D, Wang KL, Kwasnitschka T (2015b) Pleistocene to Holocene offshore tephrostratigraphy of highly explosive eruptions from the southwestern Cape Verde Archipelago. Marine Geology 369: 233-250

Federman AN, Carey SN (1980) Electron microprobe correlation of tephra layers from eastern Mediterranean abyssal sediments and the island of Santorini. Quat Res 13: 160-171

Francalanci L, Varekamp JC, Vougioukalaskis G, Defant MJ, Innocenti F, Manetti P (1995) Crystal retention, fractionation and crustal assimilation in a convecting magma chamber, Nisyros Volcano, Greece. Bull Volcanol 56: 601-620

Francalanci L, Vougioukalakis GE, Perini G, Manetti P (2005) A west-east traverse along the magmatism of the south Aegean volcanic arc in the light of volcanological, chemical and isotopic data. In: Fytikas M, Vougioukalakis GE (Eds) The south aegean active volcanic arc. Elsevier, Amsterdam: 64-112

Hardiman JC (1999) Deep sea tephra from Nisyros island, eastern Aegean Sea, Greece. In: Firth CR, McGuire WJ (eds) Volcanoes in the Quaternary. Geol Soc Lond Spec Publ 161: 69-88

Hübscher C, Ruhnau M, Nomikou P (2015) Volcano-tectonic evolution of the polygenetic Kolumbo submarine volcano/Santorini (Aegean Sea). J Volcanol Geotherm Res 291: 101-111

Johnston EN, Sparks RSJ, Phillips JC, Carey S (2014) Revised estimates for the volume of the Late Bronze Age Minoan eruption, Santorini, Greece. J Geol Soc London 171: 583-590, doi 10.1144/jgs2013-113
Karkanas P, White D, Lane CS, Stringer C, Davies W, Cullen VL, Smith VC, Ntinou M, Tsartsidou G, Kyparissi-Apostolika N (2015) Tephra correlations and climatic events between the MIS6/5 transition and the beginning of MIS3 in Theopetra Cave, central Greece. Quat Sci Rev 118: 170-181
Keller J, Ryan WBF, Ninkovich D, Altherr R (1978) Explosive volcanic activity in the Mediterranian over the past 200.000 years as recorded in deep-sea sediments. Geol Soc Am Bull 89: 591-604
Kilias SP, Nomikou P, Papanikolaou D, Polymenakou PN, Godelitsas A, Argyraki A, Carey S, Gamaletsos P, Mertzimekis TJ, Stathopoulou E, Goettlicher J, Steininger R, Betzelou K, Livanos I, Christakis C, Croff Bell K, Scoullos M (2013) New insights into hydrothermal vent processes in the unique shallow-submarine arc-volcano, Kolumbo (Santorini), Greece. Scientific Reports 3: 2421, DOI: 10.1038/srep02421
Kinvig HS, Winson A, Gottsmann J (2010) Analysis of volcanic threat from Nisyros Island, Greece, with implications for aviation and population exposure. Nat Hazards Earth Syst Sci 10: 1101-1113, doi:10.5194/nhess-10-1101-2010
Kuscu GG, Uslular G (2014) Kos-Nisyros-Yali Volcanic System: Need for a New Risk Analyses in the Area? 9th Alexander von Humboldt International Conference, Istanbul, Turkey, 24-28 March 2014 (abstract)
Kutterolf S, Freundt A, Peréz W (2008b) The Pacific offshore record of Plinian arc volcanism in Central America: 2. Tephra volumes and erupted masses. Geochem Geophys Geosys 9, doi:10.1029/2007GC001791
Kutterolf S, Freundt A, Peréz W, Mörz T, Schacht U, Wehrmann H, Schmincke H-U (2008a) The Pacific offshore record of Plinian arc volcanism in Central America: 1. Along-arc correlations. Geochem Geophys Geosyst 9, doi:10.1029/2007GC001631
Limburg EM, Varecamp JC (1991) Young pumice deposits on Nisyros, Greece. Bull Volcanol 54: 68-77
Livanos I, Nomikou P, Papanikolaou D, Rousakis G (2013) Volcanic Debris Avalanche at the SE submarine slopes of Nisyros Volcano, Greece. Geo-Marine Letters 33: 419-431
Makris J (1977) Geophysical investigation of the Hellenides. Hamburger geographische Einzelschriften 34: 1-124
Margari V, Pyle DM, Bryant C, Gibbard PL (2007) Mediterranean tephra stratigraphy revisited: Results from a long terrestrial sequence on Lesvos Island, Greece. J Volcanol Geotherm Res 163: 34-54
Mc Kenzie DP (1972) Active tectonics of the Mediterranean region. Geophys J R Astron Soc 30: 109-185
McCoy FW, Heiken G (2000) The Late-Bronze Age explosive eruption of Thera (Santorini), Greece: Regional and local effects. Geol Soc Am Spec Pap 345: 43-70
Narcisi B, Vezzoli L (1999) Quaternary stratigraphy of distal tephra layers in the Mediterranean—an overview. Global and Planetary Change 21: 31-50
Nomikou P, Carey S, Croff Bell KL, Papanikolaou D, Bejelou K, Cantner K, Sakellariou D, Peros I (2014a) Tsunami hazard risk of a future volcanic eruption of Kolumbo submarine volcano, NE of Santorini Caldera, Greece. Nat Hazards 72: 1375-1390
Nomikou P, Carey S, Papanikolaou D, Croff Bell K, Sakellariou D, Alexandri M, Bejelou K (2013a) Morphological analysis and related volcanic features of the Kolumbo submarine volcanic chain (NE of Santorini Island, Aegean volcanic arc). Zeitschrift für Geomorphologie 57: 29-47
Nomikou P, Carey S, Papanikolaou D, Croff Bell KL, Sakellariou D, Alexandri M, Bejelou K (2012) Submarine volcanoes of the Kolumbo volcanic zone NE of Santorini Caldera, Greece. Global Planet Change 90-91: 135-151
Nomikou P, Croff Bell KL, Papanikolaou D, Livanos I, Martin JF (2013b) Exploring the Avyssos-Yali-Strongyli submarine volcanic complex at the eastern edge of the Aegean volcanic arc. Zeitschrift für Geomorphologie 57: 127-137
Nomikou P, Papanikolaou D (2011) Extension of active fault zones on Nisyros volcano across the Yali-Nisyros Channel based on onshore and offshore data. Mar Geophys Res 32: 181-192
Nomikou P, Papanikolaou D, Alexandri M, Sakellariou D, Rousakis G (2013c) Submarine volcanoes along the Aegean volcanic arc. Tectonophysics 597-598: 123-146
Nomikou P, Parks MM, Papanikolaou D, Pyle DM, Mather TA, Carey S, Watts AB, Pauletto M, Kalnins ML, Livanos I, Bejelou K, Simou E, Peros I (2014b) The emergence and growth of a submarine volcano: The Kameni islands, Santorini (Greece). Geo Res J 1-2: 8-18
Papazachos BC, Dimitriadis ST, Panagiotopoulos DG, Papazachos CB, Papadimitriou EE (2005) Deep structure and active tectonics of the southern Aegean volcanic arc. In: Fytikas M, Vougioukalakis GE (Eds) The South Aegean active volcanic arc. Elsevier, Amsterdam: 4-64
Parks MM, Biggs J, England P, Mather TA, Nomikou P, Palamartchouk K, Papanikolaou X, Paradissis D, Parsons B, Pyle DM, Raptakis C, Zacharis V (2012) Evolution of Santorini Volcano dominated by episodic and rapid fluxes of melt from depth. Nature Geoscience 5: DOI: 10.1038/NGEO1562
Pyle DM, Elliott JR (2006) Quantitative morphology, recent evolution, and future activity of the Kameni islands volcano, Santorini, Greece. Geosphere 2: 253-268
Pyle DM, Margari V (2009) Reply: Correlation of a widespread Pleistocene tephra marker from the Nisyros–Yali volcanic complex, Greece. J Volcanol Geotherm Res 181: 251-254
Satow C, Tomlinson EL, Grant KM, Albert PG, Smith VC, Manning CJ, Ottolini L, Wulf S, Rohling EJ, Lowe JJ, Blockley SPE, Menzies MA (2015) A new contribution to the Late Quaternary tephrostratigraphy of the Mediterranean: Aegean Sea core LC21. Quaternary Science Reviews 117: 96-112

Smith PE, York D, Chen Y, Evensen NM (1996) Single crystal 40Ar-39Ar dating of a Late Quaternary paroxysm on Kos, Greece: Concordance of terrestrial and marine ages. Geophys Res Lett 23: 3037-3050
St. Seymour K, Vlassopoulos D (1989) The potential for future explosive volcanism associated with dome growth at Nisyros, Aegean volcanic arc, Greece. J Volcanol Geotherm Res 37: 351-364
Tibaldi A, Pasquare FA, Papanikolaou D, Nomikou P (2008a) Discovery of a huge sector collapse at the Nisyros volcano, Greece, by on-land and offshore geological-structural data. J Volcanol Geotherm Res 177: 485-499
Tibaldi A, Pasquare FA, Papanikolaou D, Nomikou P (2008b) Tectonics of Nisyros Island, Greece, by field and offshore data, and analogue modelling. J Struct Geol 30: 1489-1506
Tomlinson EL, Arienzo I, Civetta L, Wulf S, Smith VC, Hardiman M, Lane CS, Carandente A, Orsi G, Rosi M, Müller W, Menzies MA (2012a) Geochemistry of the Phlegraean Fields (Italy) proximal sources for major Mediterranean tephras: Implications for the dispersal of Plinian and co-ignimbritic components of explosive eruptions. Geochim Cosmochim Acta 93: 102-128
Tomlinson EL, Kinvig HS, Smith VC, Blundy JD, Gottsmann J, Müller W, Menzies MA (2012b) The Upper and Lower Nisyros Pumices: Revisions to the Mediterranean tephrostratigraphic record based on micron-beam glass geochemistry. J Volcanol Geotherm Res 243-244: 69-80
Tomlinson EL, Smith VC, Albert PG, Aydar E, Civetta L, Cioni R, Cubukcu E, Gertisser R, Isaia R, Menzies MA, Orsi G, Rosi M, Zanchetta G (2015) The major and trace element glass compositions of the productive Mediterranean volcanic sources: tools for correlating distal tephra layers in and around Europe. Quat Sci Rev 118: 48-66
Vespa M, Keller J, Gertisser R (2006) Interplinian explosive activity of Santorini volcano (Greece) during the past 150,000 years. J Volcanol Geotherm Res 153: 262-286
Vinci A (1985) Distribution and chemical composition of tephra layers from Eastern Mediterranean abyssal sediments. Marine Geology 64: 143-155
Volentik A, Vanderkluysen L, Principe C (2002) Stratigraphy of the caldera walls of Nisyros volcano, Greece. Eclogae geol Helv 95: 223-235
Vougioukalakis GE, Fytikas M (2005) Volcanic hazards in the Aegean area, relative risk evaluation, monitoring and present state of the active volcanic centers. In: Fytikas M, Vougioukalakis GE (Eds) The south Aegean active volcanic arc. Elsevier, Amsterdam: 161-183
Wulf S, Keller J, Paterne M, Mingram J, Lauterbach S, Opitz S, Sottili G, Giaccio B, Albert PG, Satow C, Tomlinson EL, Viccaro M, Brauer A (2012) The 100-133 ka record of Italian explosive volcanism and revised tephrochronology of Lago Grande di Monticchio. Quat Sci Rev 58: 104-123
Wulf S, Kraml M, Keller J (2008) Towards a detailed distal tephrostratigraphy in the Central Mediterranean: the last 20,000 yrs record of Lago Grande di Monticchio. J Volcanol Geotherm Res 177: 118-132
Wulf S, Kraml M, Keller J, Negendank JFW (2004) Tephrochronology of the 100 ka lacustrine sediment record of Lago Grande di Monticchio (southern Italy). Quaternary International 122: 7-30
Wulf S, Kraml M, Kuhn T, Schwarz M, Inthorn M, Keller J, Kuscu I, Halbach P (2002) Marine tephra from the Cape Riva eruption (22 ka) of Santorini in the Sea of Marmara. Marine Geology 183: 131-141
Zhu L, Mitchell BJ, Akyol N, Cemen I, Kekovali K (2006) Crustal thickness variations in the Aegean region and implications for the extension of continental crust. J Geophys Res 111: doi: 10.1029/2005JB003770